Supporting Information (SI)

Systemic immunotherapy with micellar resiquimod-polymer conjugates triggers a robust antitumor response in a breast cancer model

Hamilton Kakwere, Hua Zhang, Elizabeth S. Ingham, Marina Nura-Raie, Spencer K. Tumbale, Riley Allen, Sarah M. Tam, Bo Wu, Cheng Liu, Azadeh Kheirolomoom, Brett Z. Fite, Asaf Ilovitsh, Jamal S. Lewis and Katherine W. Ferrara[*]

1. Materials

The alkyne functionalized hyperbranched polyester was prepared following the procedure previously reported by us [1]-[2]. Boltorn H40 (Aldrich) was purified by precipitation from acetone/diethyl ether and dried under vacuum at room temperature before use. Azido−dPEG$_{12}$−NHS ester (Quantabiodesign), Azido-dPEG$_{12}$-acid (Quantabiodesign), triethylamine, TEA (Aldrich), dimethylamino pyridine (DMAP) (Aldrich), pHrodo red succinimidyl ester (Thermofisher), Di-*tert*-butyl dicarbonate (Fisher), *tert*-butanol (Acros Organics), (1-Cyano-2-ethoxy-2-oxoethylidenaminooxy)dimethylamino-morpholino-carbenium hexafluorophosphate, COMU (Aldrich), 7-Methyl-1,5,7-triazabicyclo[4.4.0]dec-5-ene, MTBD (Aldrich), diisopropylethylamine, DIPEA (Aldrich), trifluoroacetic acid, TFA (Alfa Aesar), thioanisole (Aldrich), anhydrous *N,N*-Dimethylformamide on molecular sieves (Acros Organics), *N*-(3-Dimethylaminopropyl)-*N*′-ethylcarbodiimide hydrochloride, EDC.HCl (Aldrich), *N*-hydroxybenzotriazole, Oxyma (Novabiochem) and the anti-PD1 checkpoint inhibitor (aPD-1)(BioX Cell) were used as received. All other solvents were purchased from Fisher at the highest purity available and used as received.

The *neu deletion* (NDL) metastatic mammary cancer line was a generous gift from the Alexander Borowsky Laboratory (UC Davis, Davis, CA). RAW-Blue ™ macrophages were purchased from Invivogen.

All animal experiments were performed under a protocol approved by the Institutional Animal Care and Use Committee (IACUC) of the University of California, Davis. To obtain the subcutaneous NDL metastatic tumor model of breast cancer, 6-9 weeks old female FVB mice were used (Charles River, Wilmington, MA). NDL tumor chunks obtained from a donor mouse that was sacrificed were surgically implanted bilaterally into the left and right flank fat pad of each mouse. At the time of surgery, animals were maintained anesthetized with 3% isoflurane (in oxygen, flow rate: 2 L min^{-1}).

2. Characterization

2.1. Electrospray ionization mass spectrometry

Mass spectrometry was conducted using a Thermo Electron LTQ-Orbitrap mass spectrometer and XCalibur data processing and instrument control software. Samples of appropriate concentration were made up in water/acetonitrile/TFA (50/50/0.1) v/v/v or DMF/water/TFA (50/50/0.1) v/v/v before injection into the electrospray ionization unit at 0.2 mL min^{-1} using a mobile phase of water with 0.1% formic acid (solvent A) and acetonitrile (solvent B) (50% A and 50% B) . The electrospray voltage was 4.5 kV, the sheath gas was nitrogen at 15 arbitrary units, and the heated capillary was set at (275 °C). High-resolution data was acquired at 100K FWHM in centroided mode with the lockmass feature which typically results in <2ppm mass accuracy.

2.2. Matrix-assisted laser desorption/ionization time of flight mass spectrometry (MALDI-TOF-MS)

MALDI-TOF mass spectrometry experiments were undertaken using a Bruker UltraFlextreme mass spectrometer equipped with a Smartbeam-II laser, (355 nm wavelength). The accelerating voltage was 20 kV. Samples were dissolved in water/acetonitrile/TFA (1:1:0.05) v/v/v or DMF and (10 mL) of the solution were taken and mixed with 10 mL of the matrix solution. The matrix was a saturated solution of sinapic acid in water/acetonitrile/TFA (70/30/0.05) v/v/v. The matrix solution was deposited first on the stainless steel MALDI plate and left to dry followed by deposition of the sample-matrix solution on top of the dry matrix spot. After drying, data collection and analysis was carried out using the Bruker Flex analysis software.

2.3. Reverse Phase High-Performance Liquid Chromatography (RP-HPLC)

Analytical reverse-phase RP-HPLC was performed on a Varian System 2695 separations module with a a photodiode array detector and employed a Phenomenex Jupiter Proteo C12 column (250 x 4.6 mm column, 4 µm particle size, flow rate of 1 mL min^{-1}). The mobile phase consisted of eluents A (0.05% v/v TFA in water) and B (acetonitrile) for HPLC runs.Semi-Preparative RP-HPLC was performed using Varian ProStar multi-solvent delivery system with a photodiode array detector employing a Phenomenex Jupiter Proteo Semi-Prep C_{12} column (250 x 10 mm, 10 µm particle size, flow rate 3 mL min^{-1}) at room temperature. Eluent fractions were collected every 30 seconds on a Varian 701 fraction collector. The mobile phase consisted of eluents A (0.05% v/v TFA in water) and B (acetonitrile) for HPLC runs. For purifying boc protected products, eluent A (0.01% v/v NH_4OH in water)

2.4. Nuclear Magnetic Resonance (NMR)

NMR analyses were carried out on Bruker Ultra Shield Avance 500 or 800 spectrometers. NMR analyses, analyses were conducted in various deuterated solvents as specified in the figure captions.

2.5. Fourier transform infra-red (FT-IR)

Solid and liquid samples were analyzed using a Bruker Tensor 27 FT-IR spectrometer equipped with an attenuated total reflectance (ATR) accessory. For pure samples, the number of scans per sample was set at 64.

For samples in solution, 25 mL of the reaction solution was placed on the ATR accessory and the solvent was slowly evaporated to form a thin film before scanning. Spectra were averages of 512 scans, recorded at a resolution of 4 cm^{-1} at room temperature.

2.6. Size exclusion chromatography (SEC)

SEC was used to determine the molecular weight of the polymers. SEC analyses were carried out at 60 ºC using an Ultimate 3000 SEC system equipped with a guard column and two Agilent PolarGel-M columns (molecular weight range of 500-2 000 000 g mol^{-1}) attached to a differential refractive index (DRI) detector and a variable wavelength UV-vis detector. The flow rate of the system was set at (1 mL min^{-1}) and the eluent was DMF with 0.25% (w/v) LiBr and triethylamine 5% (v/v). The SEC system was calibrated using Agilent narrow molecular weight distribution polystyrene standards.

2.7. Dynamic Light Scattering (DLS)

Particle size measurements were carried out by dynamic light scattering (DLS) using a Malvern Instruments Zetasizer Nano series instrument. The system was allowed to equilibrate for 3 min

before measurements were made and at least three replicate measurements were made for each sample.

2.8. Ultra-violet visible (UV-vis) spectrometry

UV-vis spectra were obtained using the NanoDrop 200 (Fisher Scientific).

2.9. Flow cytometry

(i) Nanoparticle uptake studies: The Cy7 cellular fluorescence was analyzed with a FACScan flow cytometer (BD Biosciences, San Jose CA) and FlowJo v10 software (Tree Star Inc., Ashland OR).

(ii) Maturation studies: Data acquisition was performed using (Attune NxT flow cytometer, Life Technologies) and the geometric fluorescent intensities as well as the percent of positively stained cells were determined. More than 10,000 events were acquired for each sample and data analysis was performed using FCS Express version 4 (De Novo Software, Los Angeles, CA).

2.10. Statistical Analysis

Statistical analyses were performed using using Prism (Version 7, GraphPad, La Jolla, CA).

3. Supplementary figures

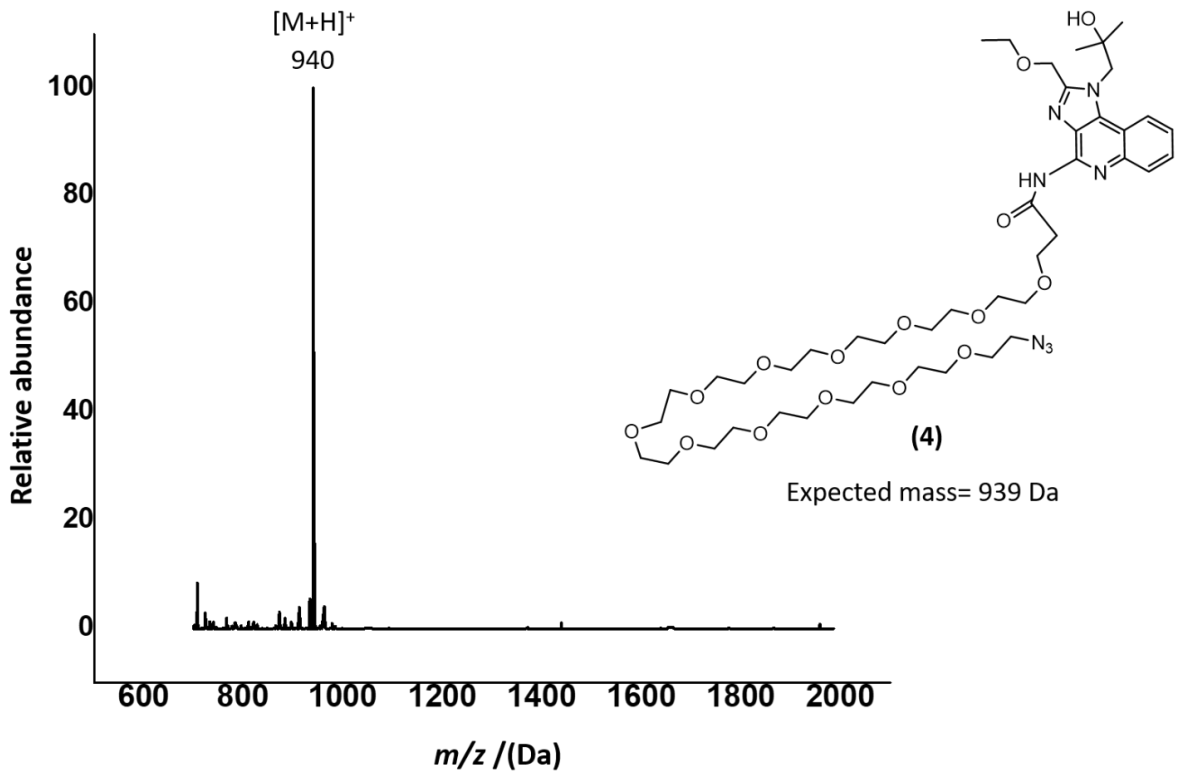

Figure S1. Mass spectrum of azido PEG- resiquimod amide conjugate **(4)**.

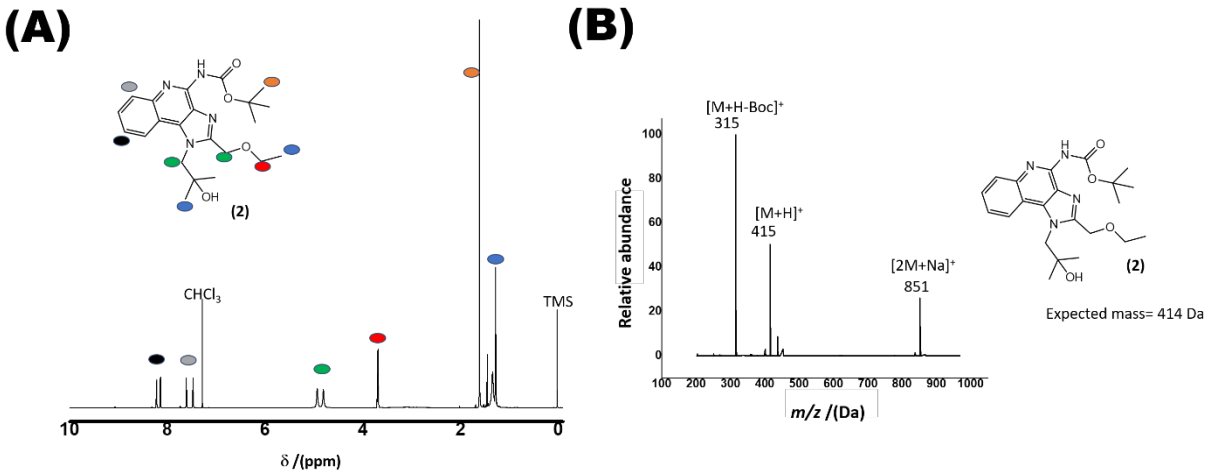

Figure S2. ^{1}H NMR spectrum and mass spectrum of (**2**) (A and B). The NMR solvent used is *d*-chloroform.

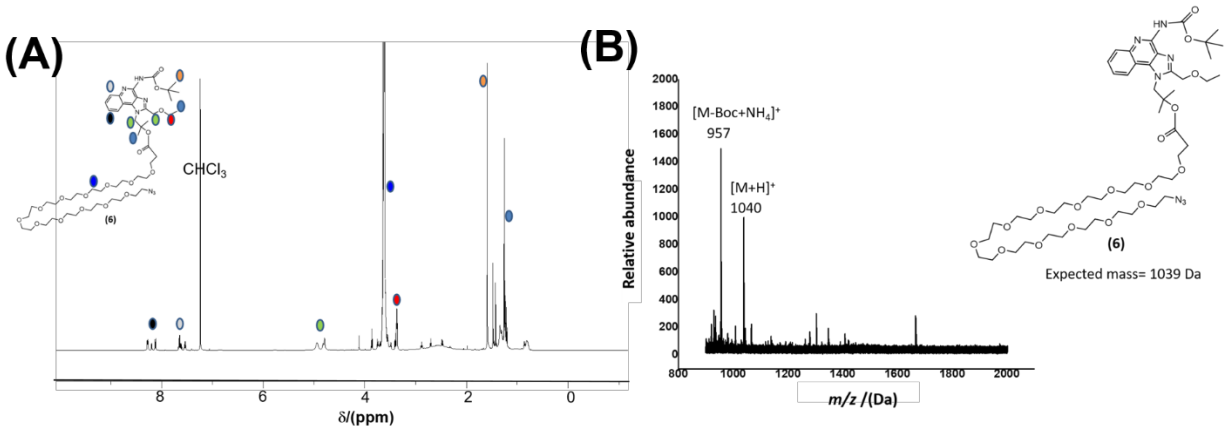

Figure S3. ^{1}H NMR and mass spectrum (A and B) of azido PEG- resiquimod ester conjugate **(6)**.

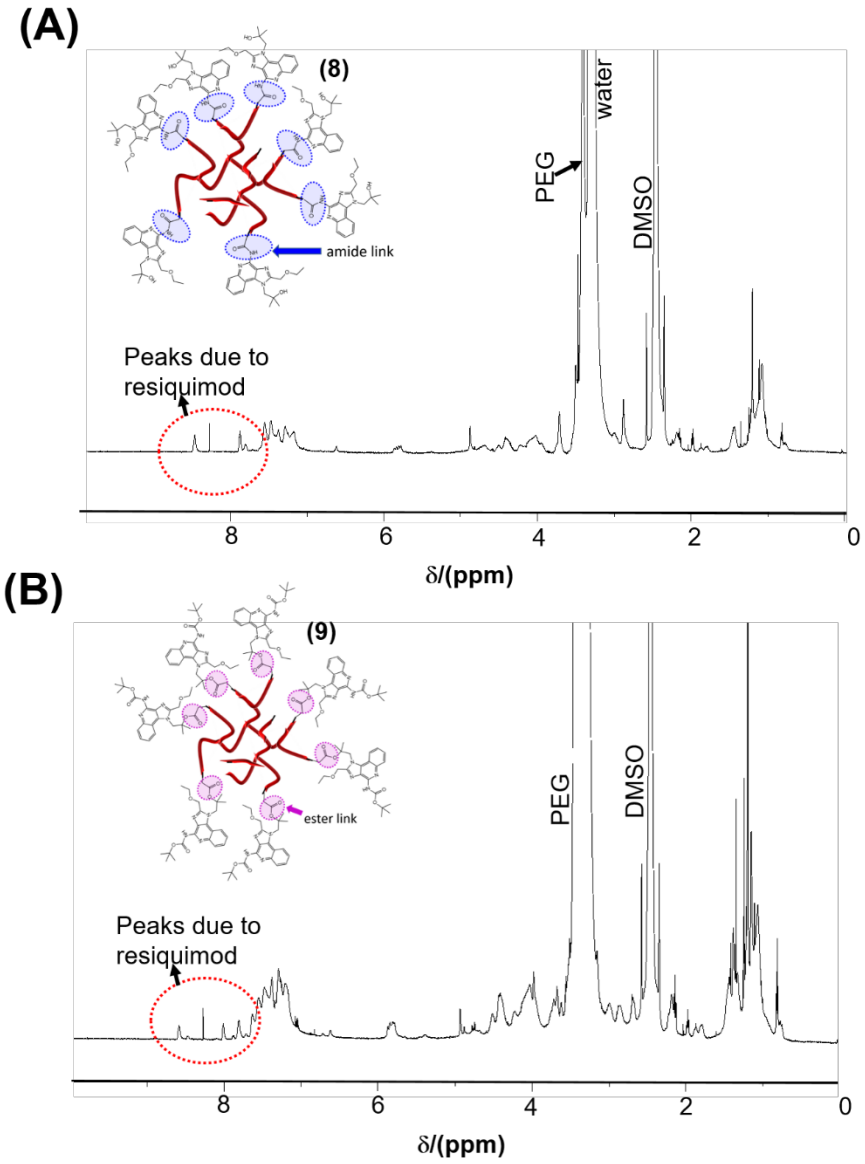

Figure S4. ^{1}H NMR spectra of the amphiphilic resiquimod-polymer conjugates **(8)** (A) and **(9)** (B). The NMR solvent used is *d*-DMSO.

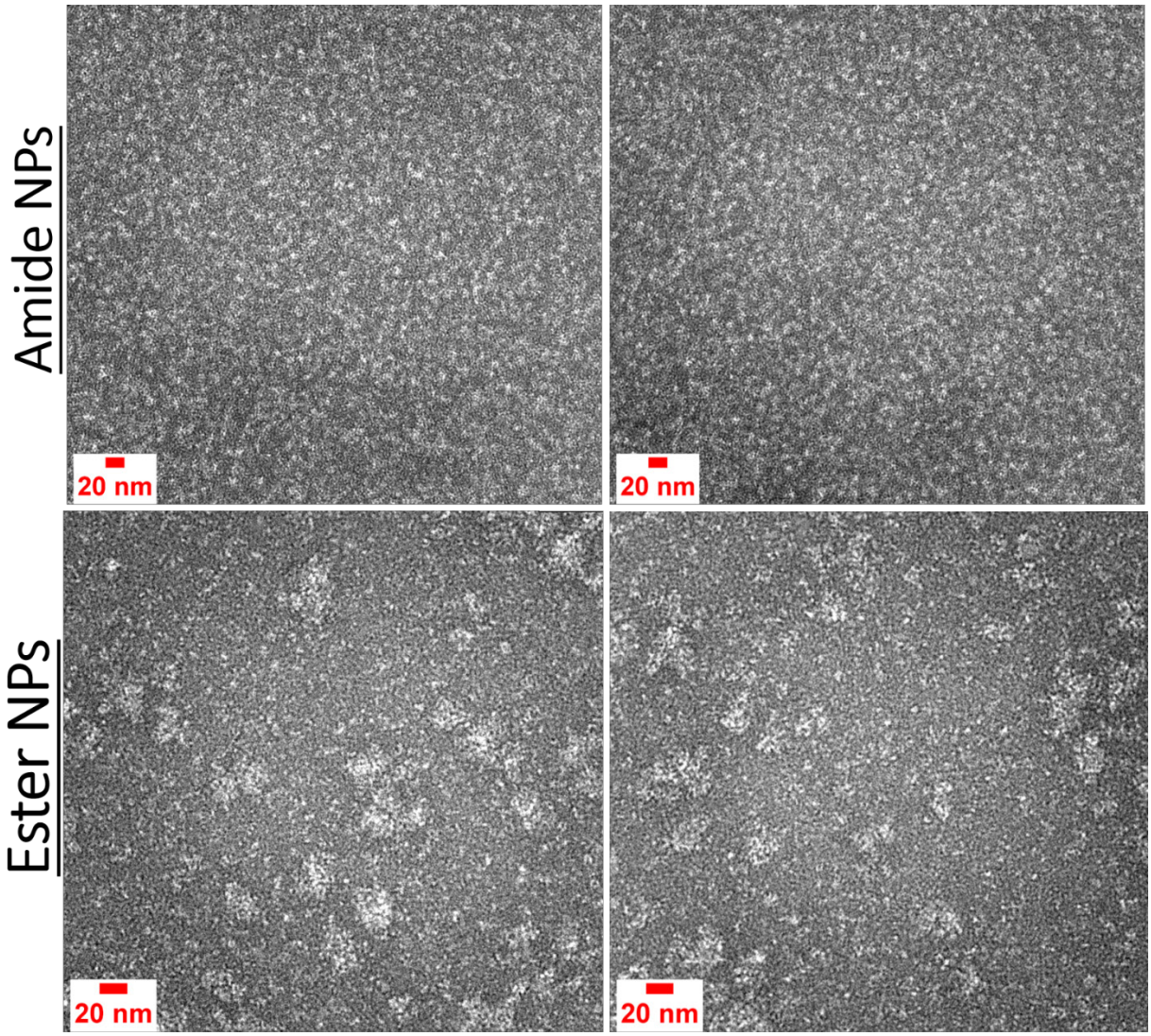

Figure S5. TEM images of the nanoparticles formed from amphiphilic resiquimod-polymer conjugates **(8)** and **(9)**. The images for each sample are from different parts of the grid.

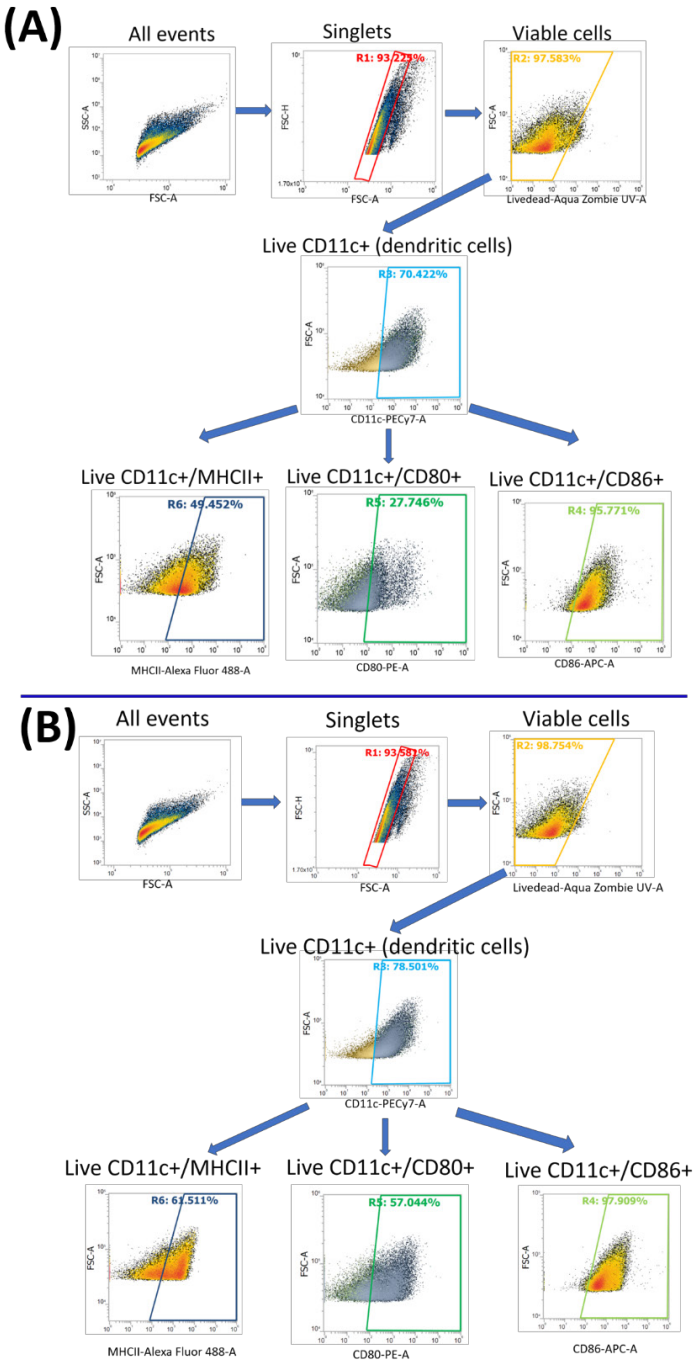

Figure S6. Flow cytometry gating strategy for the dendritic cell (DC) maturation experiment (examples shown, immature DCs (A) and DCs incubated with resiquimod (B)). The cell populations were gated based on singlets then only live cells were selected using UV Zombie dye staining. Cells were further chosen according to the cell marker CD11c for DCs. DC populations were then analyzed for other surface expressions. All the positive staining gates were set according to Fluorescence Minus One (FMO) controls.

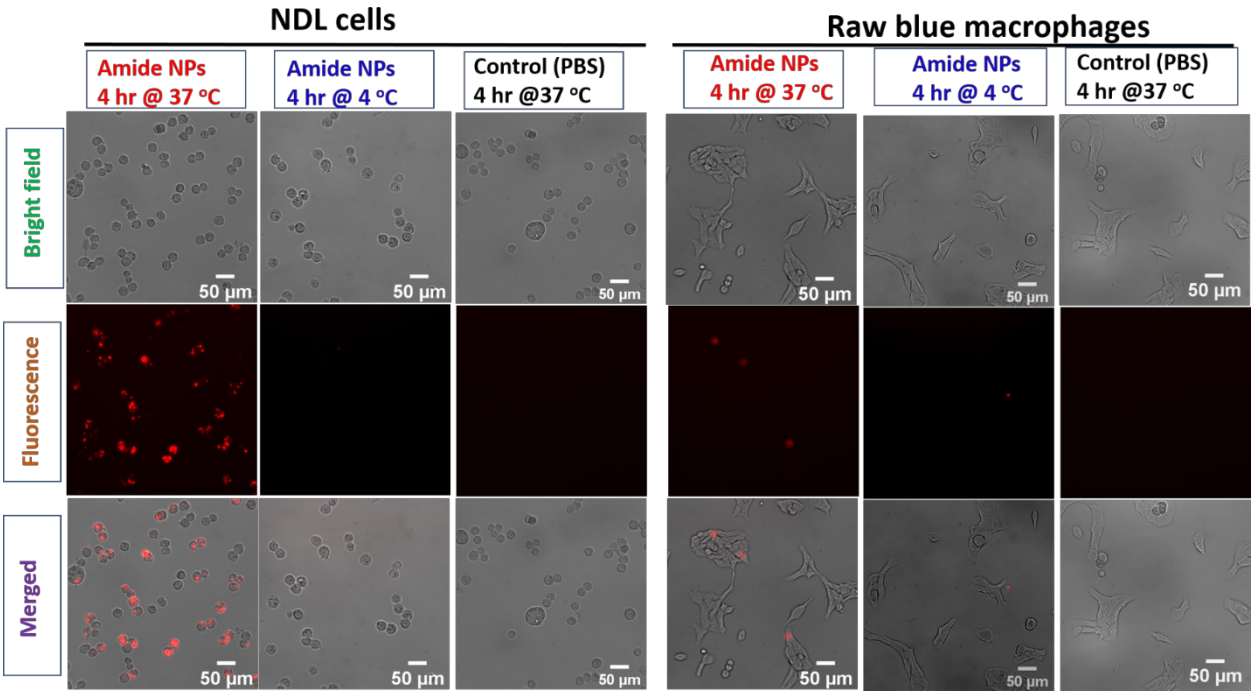

Figure S7. Uptake of pHrodo-red labeled nanoparticles by NDL cells and RAW Blue macrophages obtained at 4 hr (37 °C and 4 °C) via microscopy with NPs visible (red signal) in the fluorescence channel and merged channel. The pHrodo-red fluoresces in lysosomal compartments. Image scale bars are 50 µm.

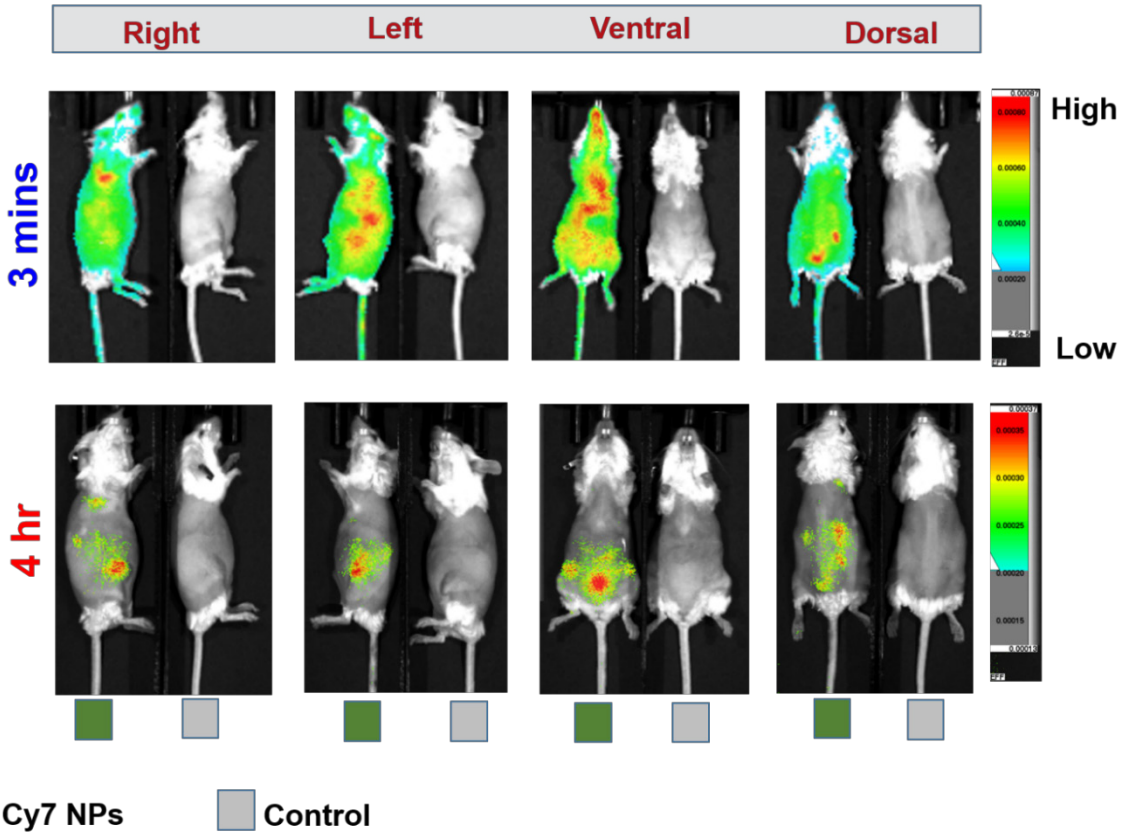

Figure S8. Biodistribution studies of Cy7-labelled NPs following injection via the mouse tail vein. Fluorescence images acquired using the SPECTRAL LAGO X, 3 min post injection and 4 hr later.

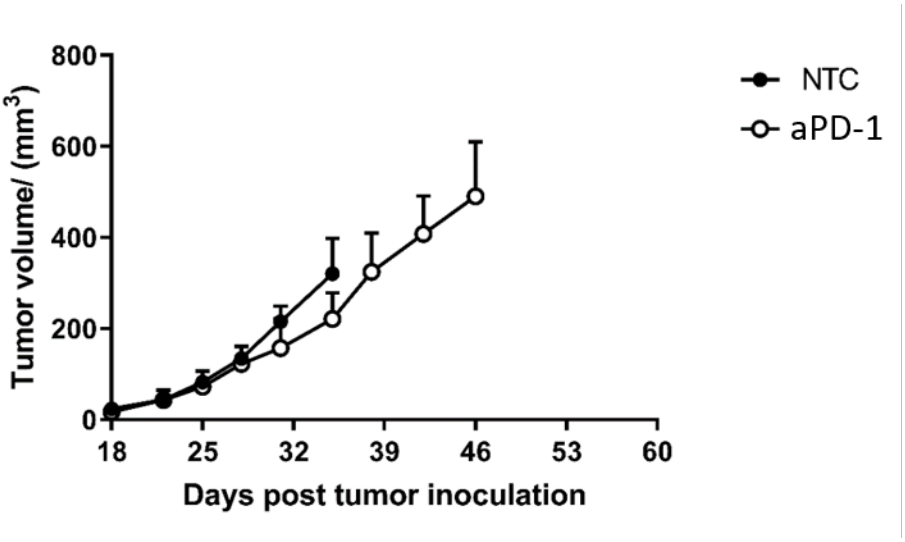

Figure S9. Study confirming aPD-1 alone is ineffective at slowing tumor growth in mice implanted with breast cancer tumors (NDL cell line). Mice (*N*=4) with pre-established bilateral breast cancer tumors ca.3 mm in size were treated with aPD-1 only on days 18, 22 and 26 post tumor inoculation which was administered intraperitoneally (i.p.). The tumor volumes ± standard deviations are averages of all tumors (*N*=8) per time point. NTC = untreated mice (no treatment control).

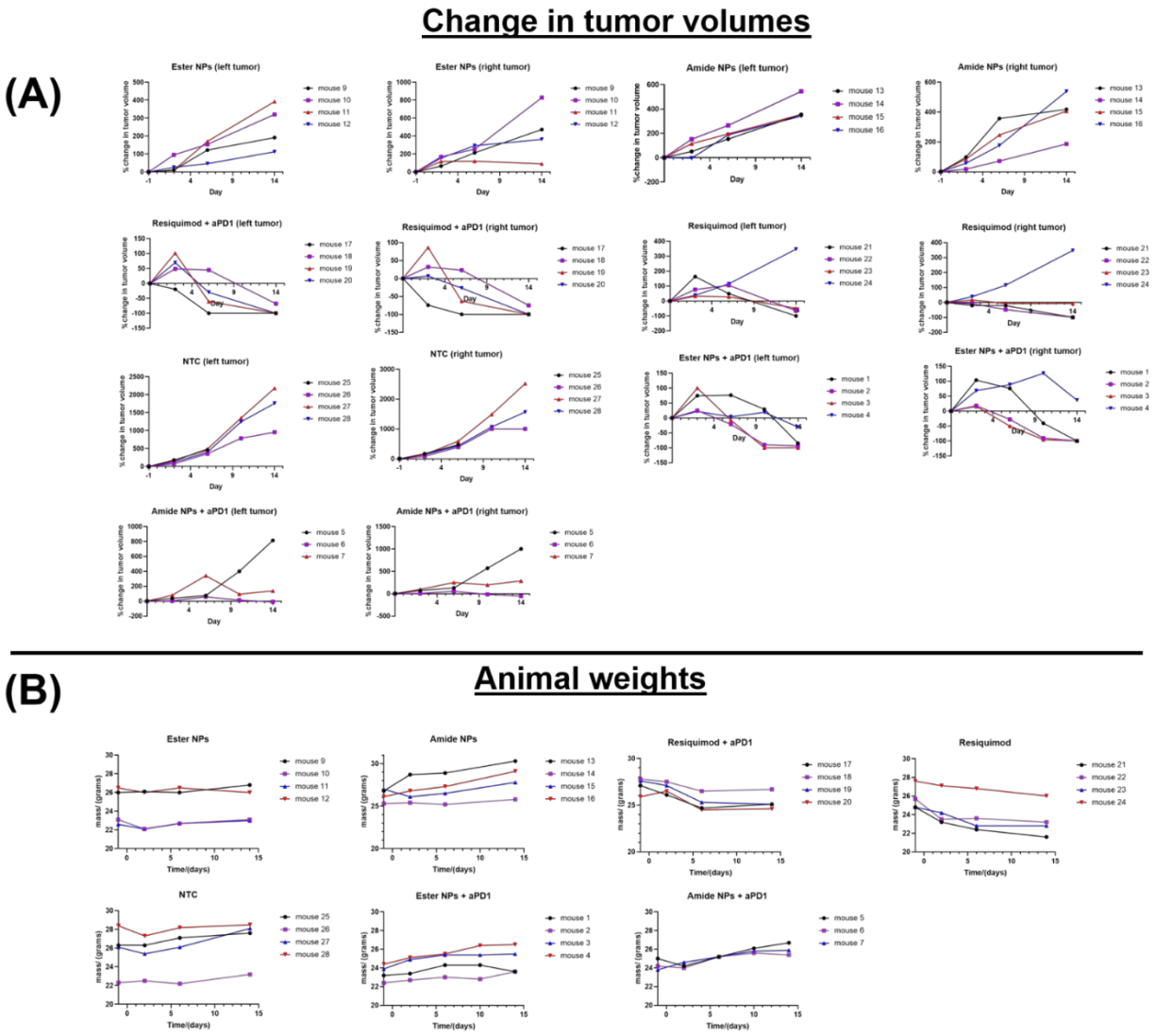

Figure S10. Change in tumor volumes of individual tumors (*N*=4) (A) and animal weights for the treatment groups studied with mice inoculated with NDL mammary carcinoma cells in both left and right flanks (B).

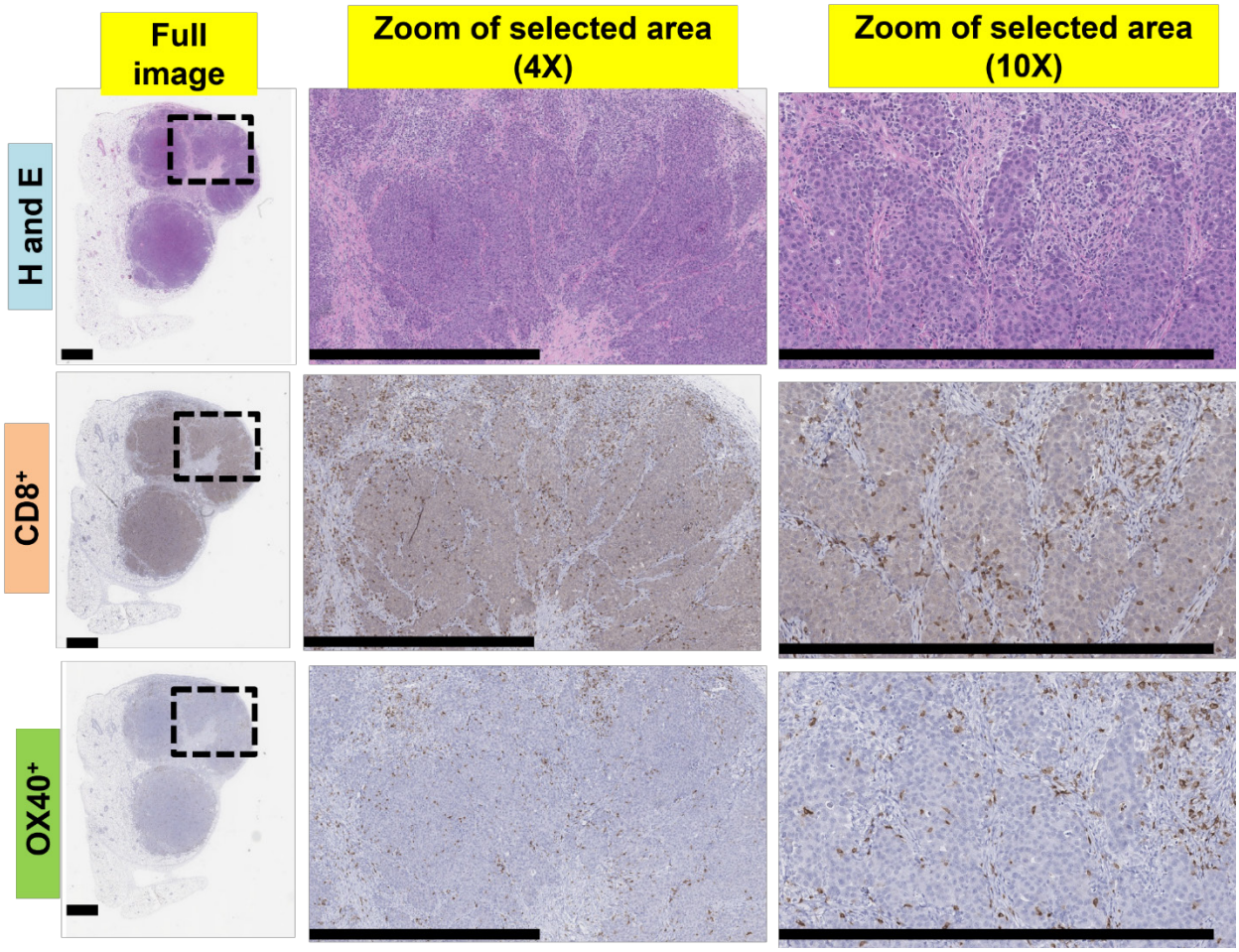

Figure S11. For mice treated with resiquimod without aPD-1, histology images showing hematoxylin and eosin (H&E)-stained tumor tissues (purple-pink), $CD8^+$ T-cell stained tissues (brown spots). The faint pink-purple color around the tumors in H&E is dead/dying tumor tissue which appears as faint gray in the $CD8^+$ T-cell images. The dotted outlines represent areas that are magnified in the subsequent series of figures. Black scale bars are 1 mm.

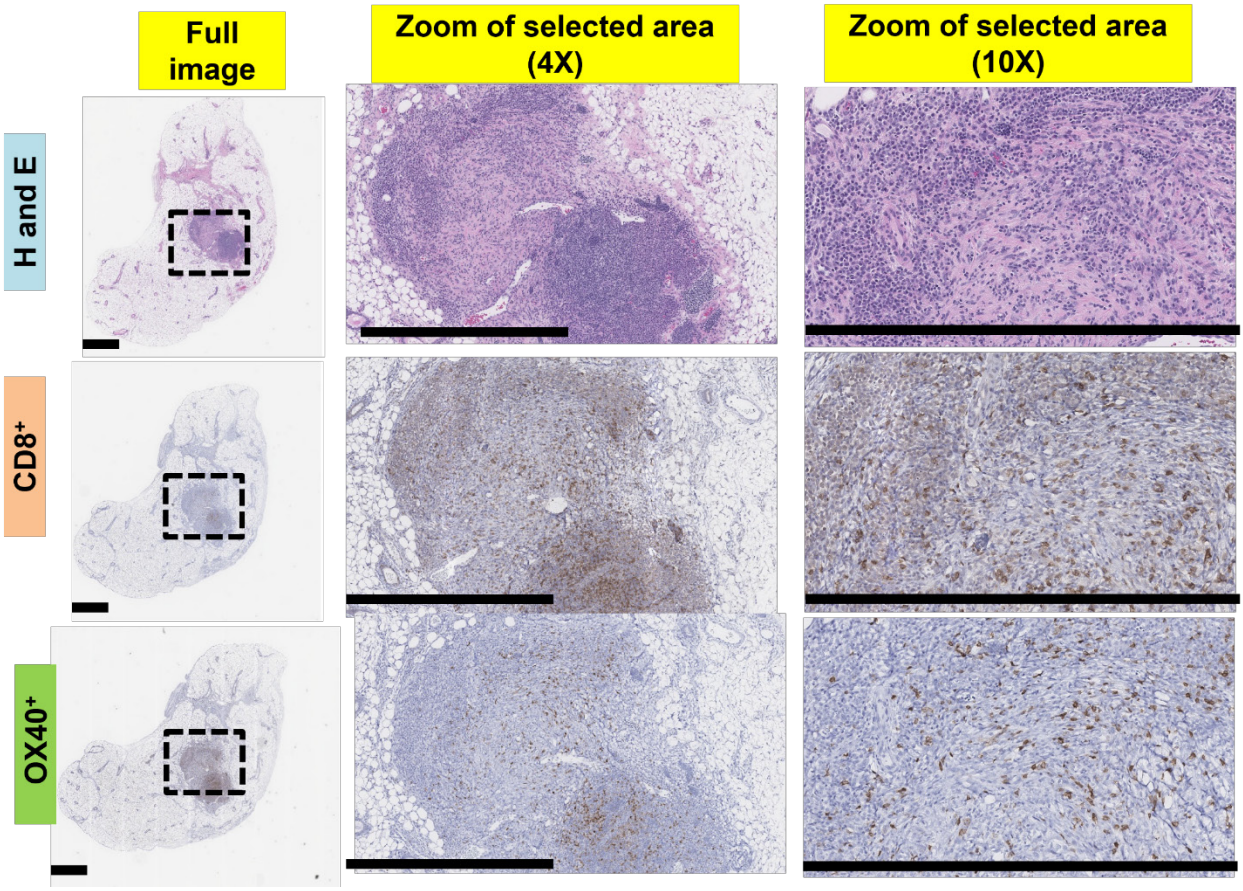

Figure S12. For mice treated with resiquimod in combination with aPD-1, histology images showing hematoxylin and eosin (H&E)-stained tumor tissues (purple-pink), $CD8^+$ T-cell stained tissues (brown spots). The faint pink-purple color around the tumors in H&E is dead/dying tumor tissue which appears as faint gray in the $CD8^+$ T-cell images. The dotted outlines represent areas that are magnified in the subsequent series of figures. Black scale bars are 1 mm.

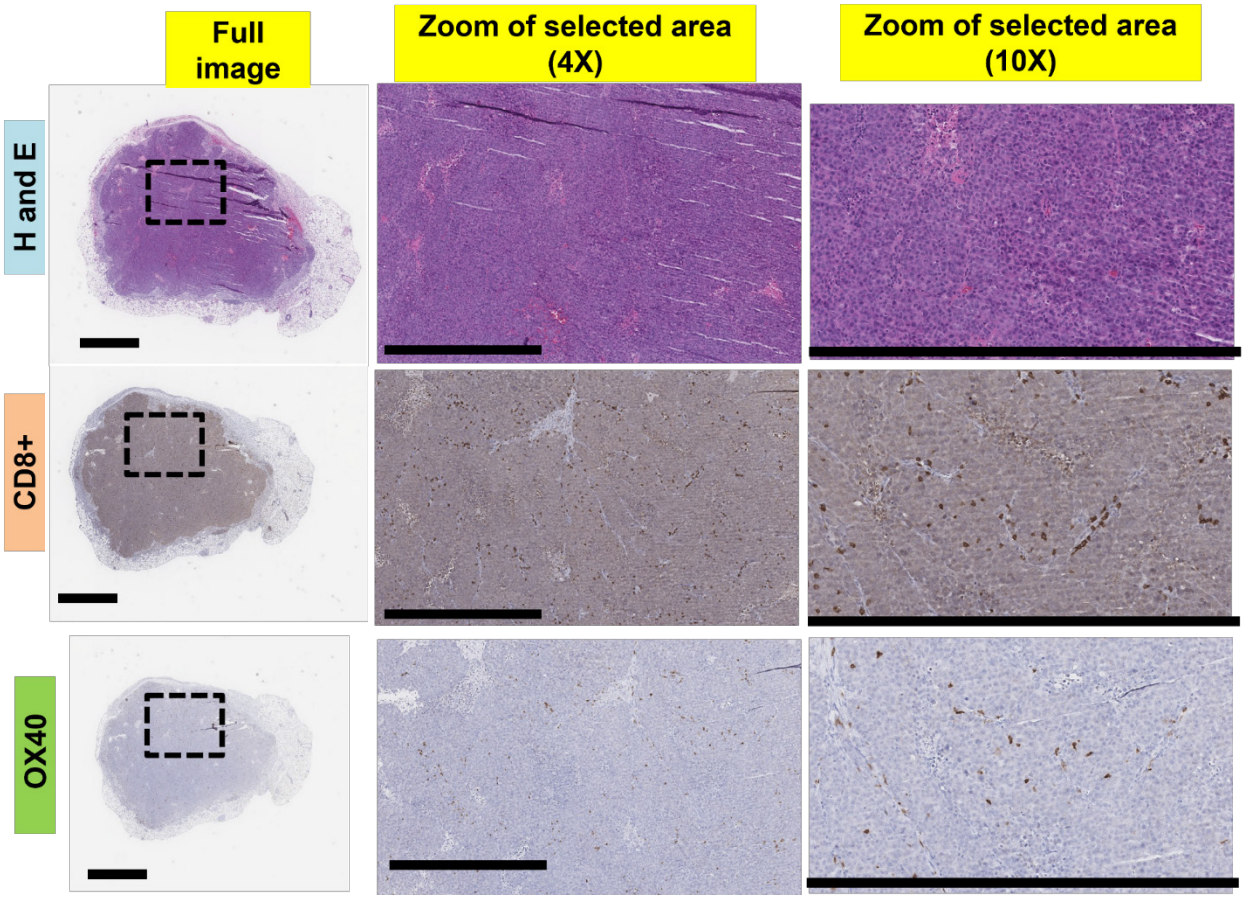

Figure S13. For mice treated with ester NPs without aPD-1, histology images showing hematoxylin and eosin (H&E)-stained tumor tissues (purple-pink), $CD8^+$ T-cell stained tissues (brown spots). The faint pink-purple color around the tumors in H&E is dead/dying tumor tissue which appears as faint gray in the $CD8^+$ T-cell images. The dotted outlines represent areas that are magnified in the subsequent series of figures. Black scale bars are 1 mm.

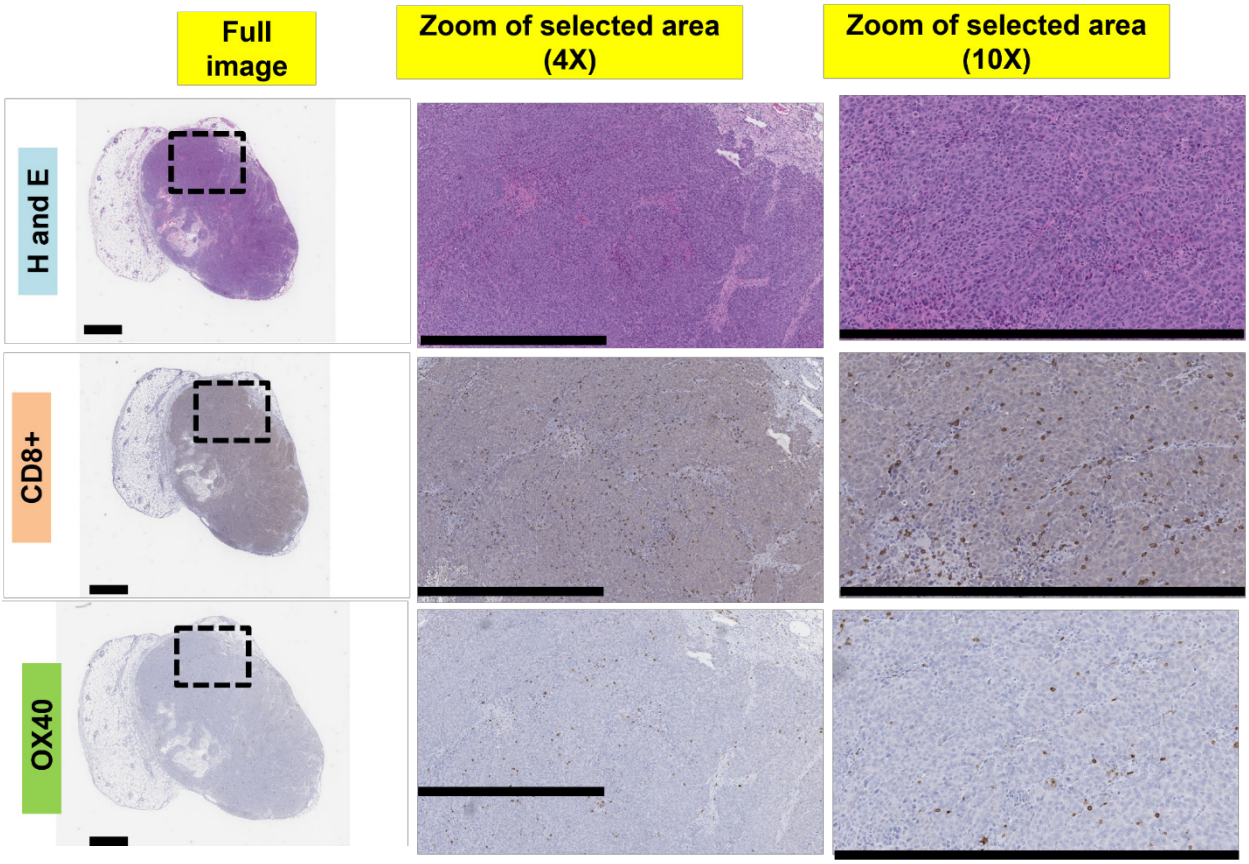

Figure S14. For mice treated with amide NPs without aPD-1, histology images showing hematoxylin and eosin (H&E)-stained tumor tissues (purple-pink), $CD8^+$ T-cell stained tissues (brown spots). The faint pink-purple color around the tumors in H&E is dead/dying tumor tissue which appears as faint gray in the $CD8^+$ T-cell images. The dotted outlines represent areas that are magnified in the subsequent series of figures. Black scale bars are 1 mm.

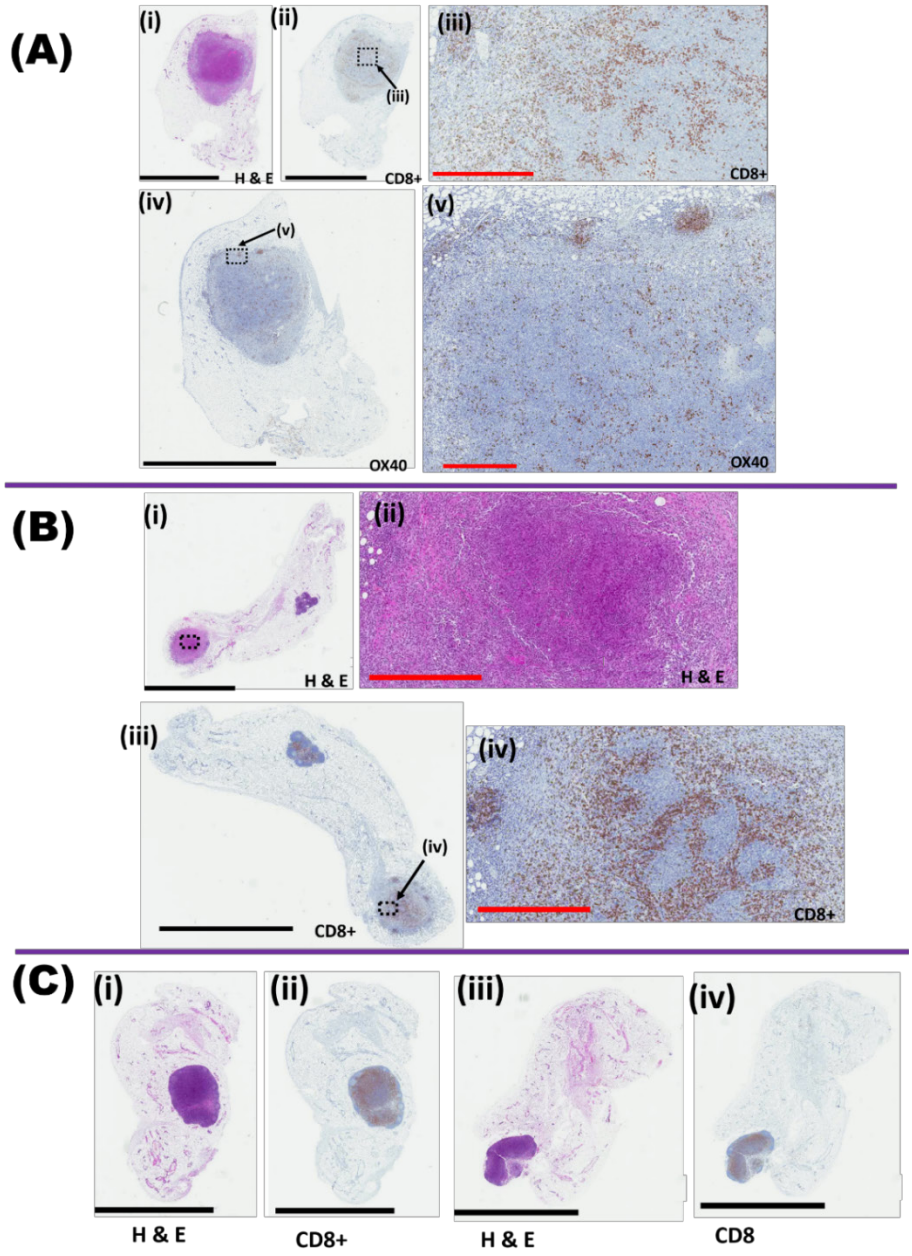

Figure S15. For mice treated with ester NPs in combination with aPD-1, histology images showing hematoxylin and eosin (H&E)-stained tissues (purple-pink), $CD8^+$ T-cell stained tissues (brown spots) and OX40 ligand stained tissues (activated T-cells, brown spots). The faint pink-purple color around the tumors in H&E is dead/dying tumor tissue which appears as faint gray in the $CD8^+$ T-cell and OX40 images. The dotted outlines represent areas that are magnified in the subsequent series of figures illustrated by the roman numerals next to the black arrows. Images show left and right tumor pairs/mouse, ((A) left and (B) right) and (C) (left (i-ii) and right (iii-iv)). For (C) (i-ii) the tumor was eliminated and the remaining tissue shown is the lymph node. Black scale bars are 5 mm while red scale bars are 0.5 mm.

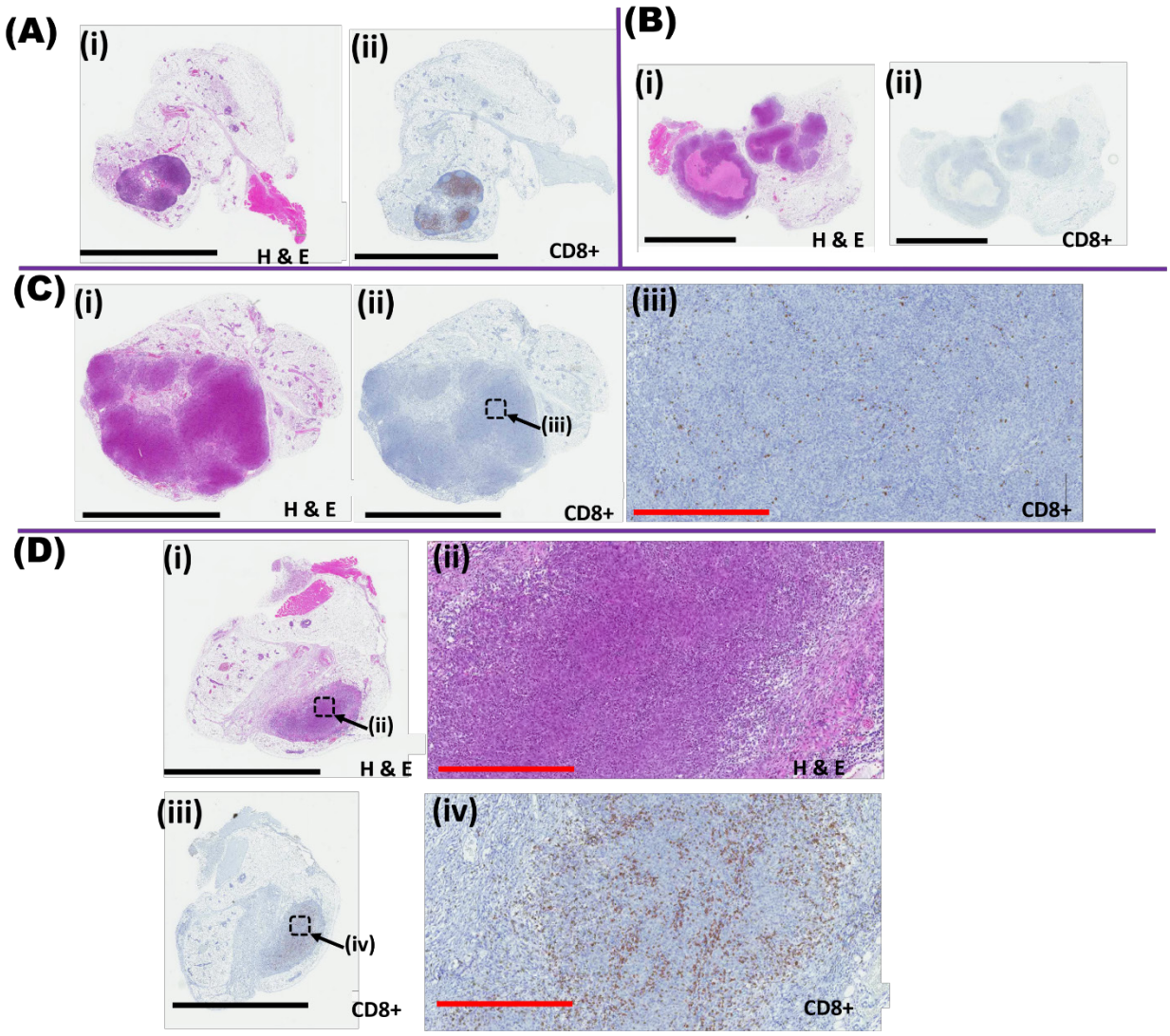

Figure S16. For mice treated with amide NPs in combination with aPD-1, histology images showing hematoxylin and eosin (H&E)-stained tumor tissues (purple-pink), $CD8^+$ T-cell stained tissues (brown spots). The faint pink-purple color around the tumors in H&E is dead/dying tumor tissue which appears as faint gray in the $CD8^+$ T-cell images. The dotted outlines represent areas that are magnified in the subsequent series of figures illustrated by the roman numerals next to the black arrows. Images show left and right fat pad pairs/mouse, ((A) left and (B) right) and ((C) left and (D) right)). For (A), the tumor was eliminated and the remaining tissue shown is the lymph node. Black scale bars are 5 mm while red scale bars are 0.5 mm.

References

[1] H. Kakwere, E. S. Ingham, R. Allen, L. M. Mahakian, S. M. Tam, H. Zhang, M. T. Silvestrini, J. S. Lewis and K. W. Ferrara, *Bioconjugate Chem.*, **2017**, *28*, 2756.
[2] H. Kakwere, E. S. Ingham, R. Allen, L. M. Mahakian, S. M. Tam, H. Zhang, M. T. Silvestrini, J. S. Lewis and K. W. Ferrara, *Biomater. Sci.*, **2018**, *6*, 2850.